

## SYNTHESIS, ANTICANCER, AND ANTIOXIDANT ACTIVITIES OF NEW AZOMETHINE DYE AND ITS CO(III) COMPLEX

*Haitham Kadhim Dakheel<sup>1</sup>, Wafaa Fadhil Abbas<sup>2</sup> & Khalid J.Al-Adilee<sup>3</sup>*

<sup>1</sup>Research Scholar, Department of Chemistry, College of Education, University of Al-Qadisiyah, Diwaniya 1753, Iraq

<sup>2</sup>Research Scholar, Ministry of Water Resources, Directorate of Cree River, Iraq

<sup>3</sup>Research Scholar, Department of Chemistry, College of Science, University of Al-Qadisiyah, Diwaniya 1753, Iraq

### ABSTRACT

In this study, azomethine ligand. (L) and its Co(III) complex was characterized by the elemental analyses, mass spectra, <sup>1</sup>H and <sup>13</sup>C NMR, infrared. Molecular structures of the azomethine ligand was determined by single crystal. X-ray diffraction studies. The harmonic oscillator model of aromaticity (HOMA) indexes for rings of synthesized azomethine ligand was calculated so order to investigate of enamine tautomer in the solid state. In ligand (L), the central shows non-aromatic character with HOMA index value of 0.4872 suggesting the keto-amine tautomer. In the solid state. In the structure of the Co(III) complexes, the central metal atom is coordinated to two phenolate oxygen atoms and two imine nitrogen atoms of two azomethine molecule in a distorted octahedral geometry. The synthesized azomethine ligand and its Co(III) complex were screened for their cytotoxicity against HeLa (human uterus carcinoma) cell lines. Finally, antioxidant capacities of the compounds were determined by different antioxidant tests such as, free radical scavenging activity, metal chelating activity, and reduction power activity.

**KEYWORDS:** Azomethine, Co(III) Complex, Antioxidant, Antiproliferative Activities, Crystal Structure

---

### Article History

**Received: 29 Sep 2020 | Revised: 07 Oct 2020 | Accepted: 09 Oct 2020**

---

### INTRODUCTION

Azomethines are organic dyes and contain group-CH=N-. Azomethines dyes are used in industry as dyes for many different textile products, colours come in different forms which include azomethines group. It has long been known that the Azomethines group has some ability to form a coordinate link with the different metal ions, and addition compounds of azobenzene with metal salts have been described [1-5]. Schiff base are capable of forming coordinate bonds with many of metal ions through azomethine nitrogen atom and additional donor atoms such as O, S and P [6-9]. A large number of Schiff bases and their complexes are of significant interest due to their diverse biological activities including anti-tumor, antibacterial, fungicidal and anti-carcinogenic [10-12]. Co(III) plays a pivotal role in cell physiology as a catalytic cofactor in the redox chemistry of mitochondrial respiration, iron absorption, free radical scavenging, and elastin cross-linking [11-15]. Cisplatin is the first member of platinum-containing anti-cancer drug. Despite highly effective in treating a various types of cancers, cisplatin has a number of side-effects such as nephrotoxicity, neurotoxicity and ototoxicity etc [16-20]. Side-effect problems of cisplatin have stimulated chemists to develop alternative anticancer drugs based on different metals. Several studies indicated that copper complexes had showed some promising results [21,22]. In our previous

papers, we reported the synthesis and characterization of new ligands and their various transition metal complexes [23–25]. Due to the importance of azo-azomethine compounds and in continuance of our interest in the syntheses of Schiff base compounds, the synthesis and spectral properties of new azomethine compounds and their metal complexes were reported herein. The proposed structure of the ligands are shown in *scheme 1*.  $^1\text{H}$ ,  $^{13}\text{C}$  NMR, IR and UV-Vis. data and elemental analyses results of the azo-azomethine compounds are presented. Additionally, anticancer and antioxidant activities of the synthesized compounds were also investigated.

## EXPERIMENTAL

### Physical Measurements

The IR spectra were obtained ( $4000\text{--}400\text{ cm}^{-1}$ ) using a Perkin Elmer spectrum 100 FT-IR spectrophotometer. NMR spectra were performed using a Bruker Advance 400 MHz Spectrometer. Melting points were obtained with a Electrothermal LDT 9200 Apparatus in open capillaries. Carbon, hydrogen and nitrogen elemental analyses were performed with a model CE-440 elemental analyzer. The UV-Vis. spectra were measured with a T80+ UV-Vis. Spectrometer PG Instruments LTD spectrometer. Data collection for X-ray crystallography was completed using a Bruker APEX2 CCD diffractometer and data reduction was performed using Bruker SAINT. SHELXTL was used to solve and refine the structures [26].

### X-Ray Crystallography

Data for (L) was collected at 150(2) K on a Bruker ApexII CCD diffractometer using Mo- $K\alpha$  radiation ( $\lambda = 0.71073\text{\AA}$ ). The structures were solved by direct methods and refined on  $F^2$  using all the reflections [27]. Hydrogen atoms bonded to the nitrogen atom in (L) was located from difference maps and refined with temperature factors riding on the carrier atom. Details of the crystal data and refinement are given **Table 1**.

### Synthesis of the Azomethine Ligand (L)

Aniline derivatives, 3-ethylaniline (0.121 g, 1 mmol), and (0.152 g, 1 mmol) 2-hydroxy-3-methoxybenzaldehyde were dissolved in 25 mL MeOH. The solution was refluxed for 3-4 h and then left at room temperature. After cooling, the azomethine dyes were obtained as red microcrystals. The microcrystals were filtered off, washed with 10 mL of cold MeOH and then dried. The purity of all azomethine dyes was evaluated by thin layer chromatography. X-ray quality crystals were obtained from the MeOH solution of the ligands by slow evaporation.

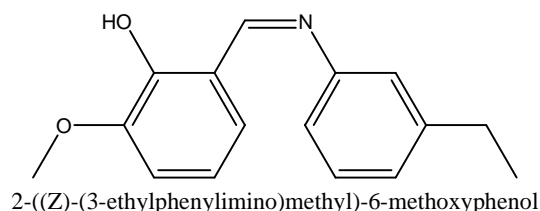


**Figure 1: The Proposed Chemical Structure Formula of the Ligand.**

(L); Orange crystals, yield: 0.33 g (79%). M.p. 113-120 °C. Elemental analyses for  $\text{C}_{16}\text{H}_{17}\text{NO}_2$  (255.31 g/mol): Calcd.: C, 75.27; H, 6.71; N, 5.49; Found: C, 75.17; H, 6.61; N, 5.39%, IR (KBr,  $\text{cm}^{-1}$ ): 3455, 2948, 1606, 1610, 1532, 1453, 1382, 1326, 1251, 1200, 1121, 987, 903, 872, 761, 670. NMR:  $^1\text{H}$  (DMSO- $d_6$  as solvent,  $\delta$  ppm.), 12.52-12.53 (*b*, 1H, phenolic OH), 9.17 (*s*, 1H, CH=N), 7.85-7.10 (11H, aromatic-H), 3.81 (*s*, 3H, -OCH<sub>3</sub>), 2.68-2.71 (*q*, 2H, CH<sub>2</sub>- of ethyl group), 1.23-1.26 (*t*, 3H, CH<sub>3</sub>- of ethyl group).  $^{13}\text{C}$  NMR (DMSO- $d_6$  as solvent,  $\delta$  ppm): 160.77, 153.6, 151.54, 126.7, 122.31, 119.47, 118.43, 32.65, 14.56.

### Synthesis of $[\text{Co}(\text{L})_2\text{Cl}_2]\cdot\text{H}_2\text{O}$

Methanolic solution of  $\text{CoCl}_3\cdot\text{H}_2\text{O}$  (0.018 g, 0.5 mmol) was added to a stirring solution of (L) (0.25 g, 1mmol) in methanol and refluxed for 2–3 h. The brown precipitate was filtered off, washed with methanol and dried in air. Yield, 0.2 g (50%). M.p. 231-239 °C. Elemental analyses for  $\text{C}_{32}\text{H}_{36}\text{ClCoN}_2\text{O}_6$  (639.02 g/mol): Calcd.: C, 60.15; H, 5.68; Co, 9.22; N, 4.38; Found: C, 60.05; H, 5.41; Co, 9.13; N, 4.29;%. IR (KBr,  $\text{cm}^{-1}$ ):3258 ,2958, 1588, 1581, 1459, 1359, 1301, 1261, 1129, 1010, 981, 912, 868, 766, 689, 616, 581.

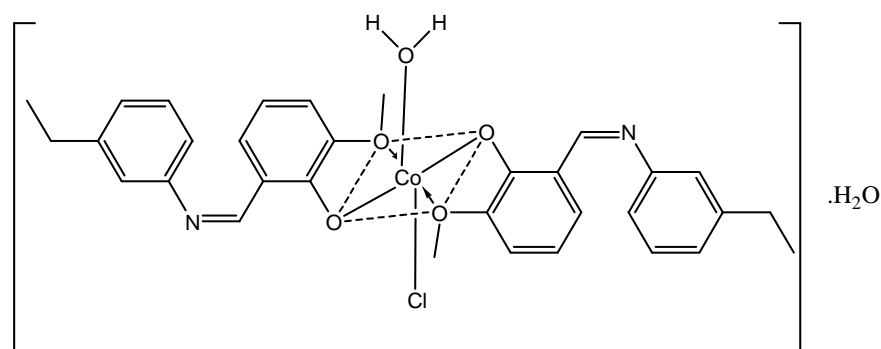


**Figure 2: The Proposed Chemical Structure Formula of the Co(III)- Complex.**

### Anticancer Studies

The Real Time Cell Analyzer-Single Plate (RTCA-SP) instrument (Roche Applied Science, Basel, Switzerland) was used to visualize the antiproliferative effects of the complexes on human cervical cancer (HeLa) cells. This instrument is a combination of four parts: an E-Plate 96, a Single Plate (SP) station that is kept in an incubator and holds the E-Plate 96, an analyzer and a computer with RTCA software. The wells of the E-Plate 96 have an inner volume of  $243\pm 5 \mu\text{L}$  and their bottoms are coated with golden electrodes. The system measures impedance differences in order to derive cell index values at time points whose intervals can be set by the operator. These impedance differences and thus the cell index values depend on the cell activity at the bottom of the wells. The higher the cell population growing at the bottom and the greater the spreading of the cells, the higher is the cell index value. This system allows the user to analyze cell behavior in a label-free environment and produces a real-time profile of the cells. The HeLa cell line was cultured in DMEM-HG supplemented with  $100 \text{ mL L}^{-1}$  heat-inactivated FBS and  $20 \text{ mL L}^{-1}$  penicillin/ streptomycin at  $37 \text{ }^\circ\text{C}$  in a humidified atmosphere of  $5\% \text{ CO}_2$ . To determine the antiproliferative effects of the synthesised compounds, HeLa cells were first detached from the tissue culture flask by treatment with trypsin/ethylenediaminetetraacetic acid solution. After detachment, the same volume of culture medium was added to this cell suspension and gently mixed. Then the suspension was partitioned into Falcon tubes and centrifuged. Meanwhile,  $50 \mu\text{L}$  of culture medium was added to each well of the E-Plate 96 and left in the hood for 15 min and in the incubator for 15 min to allow the electrodes to equilibrate with the culture medium. After this period, the E-Plate 96 was inserted into the RTCA-SP station and a background measurement was performed. Immediately afterwards, the E-Plate 96 was ejected from the station and  $100 \mu\text{L}$  of cell suspension adjusted to a concentration of  $2.5 \times 10^4$  HeLa cells per  $100 \mu\text{L}^{-1}$  was added to each well. Three wells were left blank to check if there would be an increase due to the culture medium. The plate was left in the hood for another 30 min for the cells to adhere to the bottom, after which the plate was inserted into the RTCA-SP station and a measurement lasting 80 min was started. After this period, the plate was ejected from the station and plant extracts (in dimethyl sulfoxide (DMSO)/culture medium; the final concentration of DMSO in the wells was less than  $10 \text{ mL L}^{-1}$ ) were added to the wells at three different concentrations ( $100, 50$  and  $25 \mu\text{g mL}^{-1}$ ), and the final volume of each well was adjusted to  $200 \mu\text{L}$  with culture medium.

Then the plate was connected to the station and a measurement lasting 50 h was started. The measurement was made in triplicate and results were reported as percentage of the inhibition of cell proliferation. 5-Fluorouracil was used as a standart compound.

### Antioxidant Activity

Antioxidant activities of compounds were determined by DPPH<sup>•</sup> free radical scavenging activity, Fe(III) reducing power assay, and chelating activity on ferrous ion Fe(II). DPPH<sup>•</sup> free radical scavenging activities for azomethine compound and its Co(III) complex were measured according to the method of Blois [29]. The DPPH<sup>•</sup> concentration (mM) in the reaction medium was calculated using calibration graph. Results were given IC<sub>50</sub>. The reducing activities of compounds were examined through the method of Oyaizu [30]. The reducing capacity levels of compounds, which mean to reduce the ferric-ferricyanide complex to the ferrous-ferricyanide complex of Prussian blue, were measured by reading the absorbance at 699 nm. Ferrous ion Fe(II) chelating activities of compounds were measured according to the method of Dinis *et al.* [31]. The absorbance was measured at 552 nm. EDTA was also used as positive control for metal chelator. The analyses were carried out triplicate and results were given as mean±standard deviation (SD).

## RESULTS AND DISCUSSION

### H -NMR Spectra

The <sup>1</sup>H and <sup>13</sup>C NMR spectra of azomethine ligand (L) was carried out in DMSO-d<sub>6</sub> solution and chemical shifts of the different signals are presented in experimental section. The total number of protons, calculated from the integration values, is in agreement with the expected molecular composition of the ligand. It is clear from proton NMR spectra of the synthesized ligands that broad signals lying at 12.52-12.53 ppm range give evidence that they are due to the OH group (-OH) attached to the phenyl ring of ligand (L). The azomethine (CH=N) proton of (L) exhibit a singlet at 9.17 ppm. The signal at 3.81 ppm which attributed to hydrogen proton of -OCH<sub>3</sub> group [32, 33]. In addition to this the multiple signals around 7.10–7.85 ppm are due to aromatic protons [34]. The signals of the CH<sub>2</sub> and CH<sub>3</sub> protons of the ethyl group are observed at 2.68-2.71 for (L).

### FT-IR Spectra

The infrared spectra of the free ligand (L) and its Co(III) complex was obtained using a KBr disc. The infrared spectra of the free ligand was compared with those of the Co(III) complex to access the coordination of the ligands to Co(III) ion. The FT-IR spectra of all the azomethine ligand show the absence of bands around 3455 and 3423 cm<sup>-1</sup> due to ν(OH) group, a new prominent band at 1606-1610 cm<sup>-1</sup> due to azomethine ν(CH=N) linkage appeared in all the ligand indicating that condensation between -CH=O moiety of azo-aldehyde and that of amino group of the aromatic amines has taken place resulting into the formation of the desired ligand. The displacement of -CH=N stretching frequencies from 1606-1610 cm<sup>-1</sup> in the free Schiff base ligand to lower values of 1588, 1581cm<sup>-1</sup> in the complexes indicating the coordination of azomethine nitrogen to the Co(III) ion [38]. In mononuclear Co(III) complex, two new weak bands observed at 616, 581 cm<sup>-1</sup> [39,40] region can be assigned to Cu-O stretching frequency.

### UV-Vis. Spectra

UV-Vis. spectra of Schiff base compound, existence of an absorption band above 410 nm [41]. was performed at room temperature in three organic solvents ( $\text{CHCl}_3$ , DMSO and DMF,  $10^{-5}$  M). The absorption spectra of azomethine dye are similar and exhibit two absorption bands in the solvents studied  $\text{CHCl}_3$ , DMSO and DMF. The azo group containing ligand exhibit a broad absorption band in the range of 310–398 nm. This absorption band which have a shoulder in 360–380 nm range was assigned to the  $n \rightarrow \pi^*$  transitions of the aromatic ring. The intensity of the  $n \rightarrow \pi^*$  transitions increased in the order of  $\text{CHCl}_3 \geq \text{DMF} > \text{DMSO}$ .

Absorption spectra for Co(III) complex was also recorded in DMSO solution. The complex show absorption band with a shoulder in the range of 480–570 nm. The band was assigned to  $M \rightarrow L$  charge transitions. Upon complexation with Co(III) ion, the  $\pi \rightarrow \pi^*$  transitions shifted to higher wavelengths and intensities (hyperchromic effect). In the spectra of the complexes no metal induced d-d transitions were observed in the solvents and concentrations studied.

### X-Ray Structures of (L)

The XRD study of the complex  $[\text{Co}(\text{L})_2\text{Cl}_2] \cdot \text{H}_2\text{O}$  was made with the help of X-ray diffractometer with Cu as anode material,  $K - \alpha$  [ $\text{A}^\circ$ ] = 1.54060 and the generator settings 30 mA, 40 kV. The lattice parameters were calculated. The density (d) of the complex was determined by the flotation method in a saturated solution of KBr, NaCl and benzene separately. The number of formula units per unit cell (n) is calculated from the relation  $n = dNV/M$ , where  $d$  = density of the compound,  $N$  = Avogadro's number,  $V$  = Volume of the unit cell and  $M$  = molecular weight of the complex. The value of 'n' is found to be 2.0 which agrees well with the suggested structure of the complex. The crystal system of the complex was found to be orthorhombic (Puri et al., 1993). The Scherrer equation in X-ray diffraction and crystallography is Table Selected bond angles and bond energies of the  $[\text{Co}(\text{L})_2\text{Cl}_2] \cdot \text{H}_2\text{O}$  complex. Bond angle in ( $\text{A}^\circ$ ) Bond energy in kcal/mol.

Formula which relates the size of the crystallites in a solid to the broadening of a peak in a diffraction pattern. The Debye-Scherrer equation is  $B = k\lambda / s \cos \theta$ ; where  $s$  = Crystallite size,  $k$  = wavelength of X-ray radiation (Cu  $K\alpha = 1.54060 \text{ \AA}$ ),  $k$  = constant taken as 0.94,  $\theta$  = diffraction angle ( $21.3^\circ$ ),  $B$  = Full width at half maximum height ( $0.946 \text{ \AA}$ ). The crystallite size of the complex  $[\text{Co}(\text{L})_2\text{Cl}_2] \cdot \text{H}_2\text{O}$  is found to be ( $1.607 \text{ \AA}$ ). (Patterson, 1939)

**Table 1: X-Ray Diffraction Data of the  $[\text{Co}(\text{L})_2\text{Cl}_2] \cdot \text{H}_2\text{O}$  Complex**

Observed 2 $\theta$	Calculated 2 $\theta$	d spacing	h	k	L	Difference 2 $\theta$
11.76	11.72	7.544	1	0	1	0.05
11.94	11.90	77.432	1	1	-1	0.03
12.12	12.10	7.308	1	1	1	0.01
13.11	13.11	67.745	1	4	0	0
15.78	15.71	57.635	2	2	-1	0.06

$a = 13.215 \text{ \AA}$ ,  $\alpha = 90^\circ$ , Volume (V) =  $2671.48 \text{ \AA}^3$ , Figure of merit = 7.8,  $b = 18.973 \text{ \AA}$ ,  $\beta = 90^\circ$ , Density (d) =  $0.789 \text{ g cm}^{-3}$ , Bravais lattice = p,  $c = 10.655 \text{ \AA}$ ,  $\gamma = 90^\circ$ , Number of unit Cell (n) = 2.

Probable Crystal system = Orthorhombic.

### Anticancer Activity for the Compounds

The antiproliferative activities of the azomethine compound and its Co(III) complex were investigated against HeLa cell line. The results of xCELLigence real-time monitoring of the proliferation of HeLa cells treated with different concentrations of the compounds (200, 100, 50  $\mu\text{g mL}^{-1}$ ). The cell index measurements provide a clear indication that all prepared azomethine compound and its Co(III) complex exhibit remarkable activities against HeLa cell line and their activities are higher than 5-FU at all concentrations studied (200, 100, 50  $\mu\text{g mL}^{-1}$ ). With some exceptions, anticancer properties of the synthesized compounds increased with the increase in the concentration of the compound (dose-dependent manner). Interestingly, the azomethine ligands showed higher activity at 100  $\mu\text{g mL}^{-1}$  than 200, 50  $\mu\text{g mL}^{-1}$  concentrations. The Co(III) complex exhibit anticancer properties slightly declined. It was reported that the hydroxy groups play an important role in anticancer activity [40, 41]. The results indicated that synthesized azo-azomethine ligands and their Co(III) complexes have potentials to enter clinical trials.

### Antioxidant Activity for the Compounds

In this study, the Fe(III) to Fe(II) transformation was used to evaluate the reductive ability of the azomethines and their Co(III) complex using the method of Oyaizu [30]. The antioxidant activity of antioxidants were assigned to various mechanisms, including prevention of chain initiation, binding of transition metal ion catalysts, decomposition of peroxides, prevention of continued hydrogen abstraction, reductive capacity, and radical scavenging [39]. Reducing power of the prepared compound shows low activity. Activities of the compounds were exhibited the following order: Co(III) complex > azomethines

### CONCLUSIONS

In summary, azomethine dyes were characterized and synthesized. FT-IR, mass,  $^1\text{H}$ - and  $^{13}\text{C}$  NMR spectroscopy confirms the functional groups,  $-\text{HC}=\text{N}$  imine group, of the dyes while Elemental analyses confirm the chemical composition of the synthesized compounds. The ratio of the Co(III) complex was found to be 1:2(M-L), the Co(III) ion appears to be four coordinated with the bidentate ligands. Crystal structures of the title dyes were successfully determined by single-crystal X-ray diffraction. In the biological activity studies, synthesized compounds showed higher anticancer activity than positive control (5-FU). However, the compounds exhibit low antioxidant activities at all antioxidant activity assays. According to result, synthesized compounds had high antiproliferative activity therefore the compounds may have potential to be used as anticancer agent after clinical trials.

### REFERENCES

1. I. Kostova, *Synthetic and natural coumarins as cytotoxic agents*, *Curr. Med. Chem. Anti Canc. Agents* 5 (2005) 29–46.
2. N. Obaiah, Y.D. Bodke, S. Telkar, *Synthesis of 3-[(1H-Benzimidazol-2-ylsulfanyl)(aryl)methyl]-4-hydroxycoumarin derivatives as potent bioactive molecules*, *ChemistrySelect* 5 (2020) 178–184.
3. O. Nagaraja, Y.D. Bodke, R. Kenchappa, S. Ravi Kumar, *Synthesis and characterization of 3-[3-(1H-benzimidazol-2-ylsulfanyl)-3-phenyl propanoyl]-2H-chromen-2-one derivatives as potential biological agents*, *Chem. Data Collect.* 27 (2020) 100369.

4. S. Lee, K. Sivakumar, W.S. Shin, F. Xie, Q. Wang, *Synthesis and anti-angiogenesis activity of coumarin derivatives*, *Bioorg. Med. Chem. Lett* 16 (2006) 4596–4599.
5. R.A. Ford, D.R. Hawkins, B.C. Mayo, A.M. Api, *The in vivo dermal absorption and metabolism of [4-14C] coumarin by rats and by human volunteers under simulated conditions of use in fragrances*, *Food Chem. Toxicol.* 39 (2001) 153–162.
6. B.S. Kirkiacharian, E. De Clercq, R. Kurkjian, C. Pannecouque, *New synthesis and anti-HIV and antiviral properties of 3-arylsulfonyl derivatives of 4-hydroxycoumarin and 4-hydroxyquinolone*, *Pharmaceut. Chem. J.* 42 (2008) 265.
7. C.A. Kontogiorgis, D.J. Hadjipavlou-Litina, *Synthesis and anti-inflammatory activity of coumarin derivatives*, *J. Med. Chem.* 48 (2005) 6400–6408.
8. M. Chandel, S.M. Roy, D. Sharma, S.K. Sahoo, A. Patel, P. Kumari, U.D. Patil, *Anion recognition ability of a novel azo dye derived from 4-hydroxycoumarin*, *J. Lumin.* 154 (2014) 515–519.
9. A.O. Gerasov, M.P. Shandura, Y.P. Kovtun, *Polymethine dyes derived from the boron difluoride complex of 3-acetyl-5, 7-di (pyrrolidin-1-yl)-4-hydroxycoumarin*, *Dyes Pigments* 79 (2008) 252–258.
10. A.O. Gerasov, M.P. Shandura, Y.P. Kovtun, *Series of polymethine dyes derived from 2, 2-difluoro-1, 3, 2-(2H)-dioxaborine of 3-acetyl-7-diethylamino-4-hydroxycoumarin*, *Dyes Pigments* 77 (2008) 598–607.
11. F. Karci, N. Ertan, *Synthesis of some novel hetarylazo disperse dyes derived from 4-hydroxy-2H-1-benzopyran-2-one (4-hydroxycoumarin) as coupling component and investigation of their absorption spectra*, *Dyes Pigments* 64 (2005) 243–249.
12. A. Panitsiri, S. Tongkhan, W. Radchatawedchakoon, U. Sakee, *Synthesis and anion recognition studies of novel bis(4-hydroxycoumarin) methane azo dyes*, *J. Mol. Struct.* 1107 (2016) 14–18.
13. H. Zhang, T. Yu, Y. Zhao, D. Fan, L. Chen, Y. Qiu, L. Qian, K. Zhang, C. Yang, *Crystal structure and photoluminescence of 7-(N,N-diethylamino)-coumarin-3-carboxylic acid*, *Spectrochim. Acta, Part A* 69 (2008) 1136–1139.
14. J. Keshavayya Vinodkumar, M. Pandurangappa, B.N. Ravi, *Synthesis, characterization and electrochemical investigations of azo dyes derived from 2-amino-6-ethoxybenzothiazole*, *Chem. Data Collect.* 17 (2018) 13–29.
15. M. Hagar, H.A. Ahmed, O.A. Alhaddadd, *DFT calculations and mesophase study of coumarin esters and its azoesters*, *Crystals* 8 (2018) 359.
16. Z. Ngaini, N.A. Mortadza, *Synthesis of halogenated azo-aspirin analogues from natural product derivatives as the potential antibacterial agents*, *Nat. Prod. Res.* 33 (2019) 3507–3514.
17. L. Zhang, J.M. Cole, P.G. Waddell, K.S. Low, X. Liu, *Relating electron donor and carboxylic acid anchoring substitution effects in azo dyes to dye-sensitized solar cell performance*, *ACS Sustain. Chem. Eng.* 1 (2013) 1440–1452.
18. C.Z.W. Sie, Z. Ngaini, *Incorporation of kojic acid-azo dyes on TiO<sub>2</sub> thin films for dye sensitized solar cells applications*, *J. Solar Energy* (2017) 1–10.

19. R. Węglowski, W. Piecek, A. Kozanecka-Szmigiel, J. Konieczkowska, E. Schab-Balcerzak, *Poly (esterimide) bearing azobenzene units as photoaligning layer for liquid crystals*, *Opt. Mater.* 49 (2015) 224–229.
20. M. Ozkütük, E. İpek, B. Aydın, S. Mamas, Z. Seferoglu, *Synthesis, spectroscopic, thermal and electrochemical studies on thiazolyl azo based disperse dyes bearing coumarin*, *J. Mol. Struct.* 1108 (2016) 521–532.
21. K.V. Basavarajappa, Y. Arthoba Nayaka, H.T. Purushothama, R.O. Yathisha, M.M. Vinay, B.J. Rudresha, K.B. Manjunatha, *Optical, electrochemical and current-voltage characteristics of novel coumarin based 2,4-dinitrophenylhydrazones derivatives*, *J. Mol. Struct.* 1199 (2020) 126946.
22. N.N. Ayare, H.S. Ramugade, N. Sekar, *Photostable coumarin containing azo dyes with multifunctional property*, *Dyes Pigments* 163 (2019) 692–699.
23. E. Madihlagan, B.N. Sunil, Z. Ngaini, G. Hegde, *Synthesis, liquid crystalline properties and photo switching properties of coumarin-azo bearing aliphatic chains: application in optical storage devices*, *J. Mol. Liq.* 292 (2019) 111328.
24. J. George, J.C. Prasana, S. Muthu, T.K. Kuruvilla, R.S. Saji, *Evaluation of vibrational, electronic, reactivity and Bioactivity of Propafenone-A spectroscopic, DFT and molecular docking approach*, *Chem. Data Collect* 26 (2020) 100360.
25. R. Schwalbe, L. Steele-Moore, A.C. Goodwin, *Antimicrobial Susceptibility Testing Protocols*, Crc Press, 2007, pp. 139–209.
26. P. Klahn, M. Bronstrup, *New structural templates for clinically validated and novel targets in antimicrobial drug research and development*, *Curr. Top. Microbiol. Immunol.* 398 (2016) 365–417.
27. M.C. Lourenco, M.V. de Souza, A.C. Pinheiro, M.D.L. Ferreira, R.S. Gonçalves, T.C.M. Nogueira, M.A. Peralta, *Evaluation of anti-tubercular activity of nicotinic and isoniazid analogues*, *Arkivoc* 15 (2007) 181–191.
28. N.B. Chilamakuru, V. Shankarananth, K.K. Rajasekhar, T. Singirisetty, *Synthesis, characterisation and anti-tubercular activity of some new 3,5-disubstituted-2,4-thiazolidinediones*, *Asian J. Pharmaceut. Clin. Res.* 6 (2013) 29–33.
29. T. Maniatis, *Molecular Cloning. Decontamination of Dilute Solutions of Ethidium Bromide*, 1989.
30. A.Z. El-Sonbati, G.G. Mohamed, A.A. El-Bindary, W.M.I. Hassan, M.A. Diab, S.M. Morgan, A.K. Elkholy, *Supramolecular structure, molecular docking and thermal properties of azo dye complexes*, *J. Mol. Liq.* 212 (2015) 487–502.
31. Z. Asadi, M.D. Esrafil, E. Vessally, M. Asnaashariisfahani, S. Yahyaei, A. Khani, *Erratum to "A structural study of fentanyl by DFT calculations, NMR and IR spectroscopy"* [*J. Mol. Struct.* 1128 (2017) 552–562], *J. Mol. Struct.* 1154 (2018) 8.
32. M. Pandey, S. Muthu, N.N. Gowda, *Quantum mechanical and spectroscopic (FT-IR, FT-Raman, <sup>1</sup>H, <sup>13</sup>C NMR, UV-Vis) studies, NBO, NLO, HOMO, LUMO and Fukui function analysis of 5-Methoxy-1H-benzo [d] imidazole-2 (3H)-thione by DFT studies*, *J. Mol. Struct.* 1130 (2017) 511–521.

33. N.M. Mallikarjuna, J. Keshavayya, M.R. Maliyappa, R.S. Ali, T. Venkatesh, Synthesis, characterization, thermal and biological evaluation of Cu (II), Co (II) and Ni (II) complexes of azo dye ligand containing sulfamethaxazole moiety, *J. Mol. Struct.* 1165 (2018) 28–36.
34. M.R. Maliyappa, J. Keshavayya, M. Mahanthappa, Y. Shivaraj, K.V. Basavarajappa, 6-Substituted benzothiazole based dispersed azo dyes having pyrazole moiety: synthesis, characterization, electrochemical and DFT studies, *J. Mol. Struct.* 1199 (2020) 126959.
35. J. George, J.C. Prasana, S. Muthu, T.K. Kuruvilla, S. Savanthi, R.S. Saji, Spectroscopic (FT-IR, FT-Raman) and Quantum mechanical study on N-(2,6 dimethyl phenyl)-2-[4-[2hydroxy-3-(2methoxyphenoxy)propyl]piperazinyl]acetamide, *J. Mol. Struct.* 1171 (2018) 268–278.
36. V.D. Vitnik, Z.J. Vitnik, The spectroscopic (FT-IR, FT-Raman,  $^{13}\text{C}$ ,  $^1\text{H}$  NMR and UV) and NBO analyses of 4-bromo-1-(ethoxycarbonyl) piperidine-4-carboxylic acid, *Spectrochim. Acta Mol. Biomol. Spectrosc.* 138 (2015) 1–12.
37. B. Kosar, C. Albayrak, Spectroscopic investigations and quantum chemical computational study of (E)-4-methoxy-2-[(p-tolylimino) methyl] phenol, *Spectrochim. Acta Mol. Biomol. Spectrosc.* 78 (2011) 160–167.
38. L. Sinha, O. Prasad, V. Narayan, S.R. Shukla, Raman, FT-IR spectroscopic analysis and first-order hyperpolarisability of 3-benzoyl-5-chlorouracil by first principles, *Mol. Simulat.* 37 (2011) 153–163.
39. M.S. Alam, D.U. Lee, Spectral (FT-IR, FT-Raman, UV, and fluorescence), DFT, and solid state interaction analyses of (E)-4-(3, 4-dimethoxybenzylideneamino)-1, 5-dimethyl-2-phenyl-1H-pyrazol-3 (2H)-one, *J. Mol. Struct.* 1128 (2017) 174–185.
40. J. Keshavayya Vinodkumar, I. Pushpavathi, C.T. Keerthikumar, M.R. Maliyappa, B.N. Ravi, Synthesis, characterization, computational and biological studies of nitrothiazole incorporated heterocyclic azo dyes, *Struct. Chem.* (2020).
41. J. Keshavayya Vinodkumar, Synthesis, structural investigations and in vitro biological evaluation of N, N-dimethyl aniline derivatives based azo dyes as potential pharmacological agents, *J. Mol. Struct.* 1186 (2019) 404–412

